

## Supplementary Figure S1

```

Homo sapiens      MSRPVRRNRKVVVDSYQFQESDDADEDYGRDSGPPPKKIRSSPREAKNRRRSGKNSQEDSEDSEDKDVKTKKDDSHS-----
Mouse            MSRPVRRNRKVVVDSYQFQESDDADEDYGRDSGPPPAKKIRSSPREAKNRRRSGKNSQEDSEDSEKKDVKTKKDDSHS-----
Chinese hamster  MSRPVRRNRKVVVDSYQFQESDDADEDYGRDSGPPSKKIRSSPREAKNRRRSGKNSQEDSEDSEKKDVKTKKDDSHSAEDFGSEDDDLGADD
African clawed frog MSRPVRRNRKVVVDSYQFQDSD--DEDYGKESAPPLKARRSSREVEKRRRSGKNSQEDSEDSEKKDVKTKKKEGSDAEDFGSGDDLAEGDG
Pufferfish      -----RNRKVVVNSYQFQDSD--ADEEYGDSEK--KVVHTAPHEPKLKR--SKNSQDSESDEKLSKSKNDSADDFGSDEEDNDFGEEDE
Zebrafish       MARPVRRNRKVVVNSYQFNESDDADEDYGRKEKETTKKIRAPPRENKHKK--SKNSQESEDSEKLTKSKNDSADDFGSDE-DNDFGEE

Homo sapiens      -----AEDSEDEKEDHKNVRRQQAASKAASKQREMLMEDVGSE-EEQEEDEAPFQEKDSG
Mouse            -----AEDSEDEKEDHKNVRRQQAASKAASKQREMLLEDVGSE-EEPEEDEAPFQENSG
Chinese hamster  GKADSDYESSQKSKKGKAKPDKNKRASKSRKRPAEDSEDEKEDHKNVRRQQAASKAASKQREMLMDVGSE-EEQEDEAPFQENSG
African clawed frog --KADSDYESPKRSKKGKKPTDKKRASKQRKRSAQDSDDEKHKNVRRQQAASKAVSKQREMLMGDGGSEDEEQEEDEAPFLEKDSG
Pufferfish      --DAGSDYDDKRGKAKKAKPEKPSKRGPKRRRAADSDDDREVSRK-RTVRRQAASKAVSKQREILLGDGGSEEDEQEDQEESYMDPDESG
Zebrafish       --DGGSDYGDKKAKKKGKPKVEKPGKSLKRKRGGDSDDDKEVSRKQRVRRQAASKAVSKQREILLGDGGSEEDEKDEEQAFLD-QESG

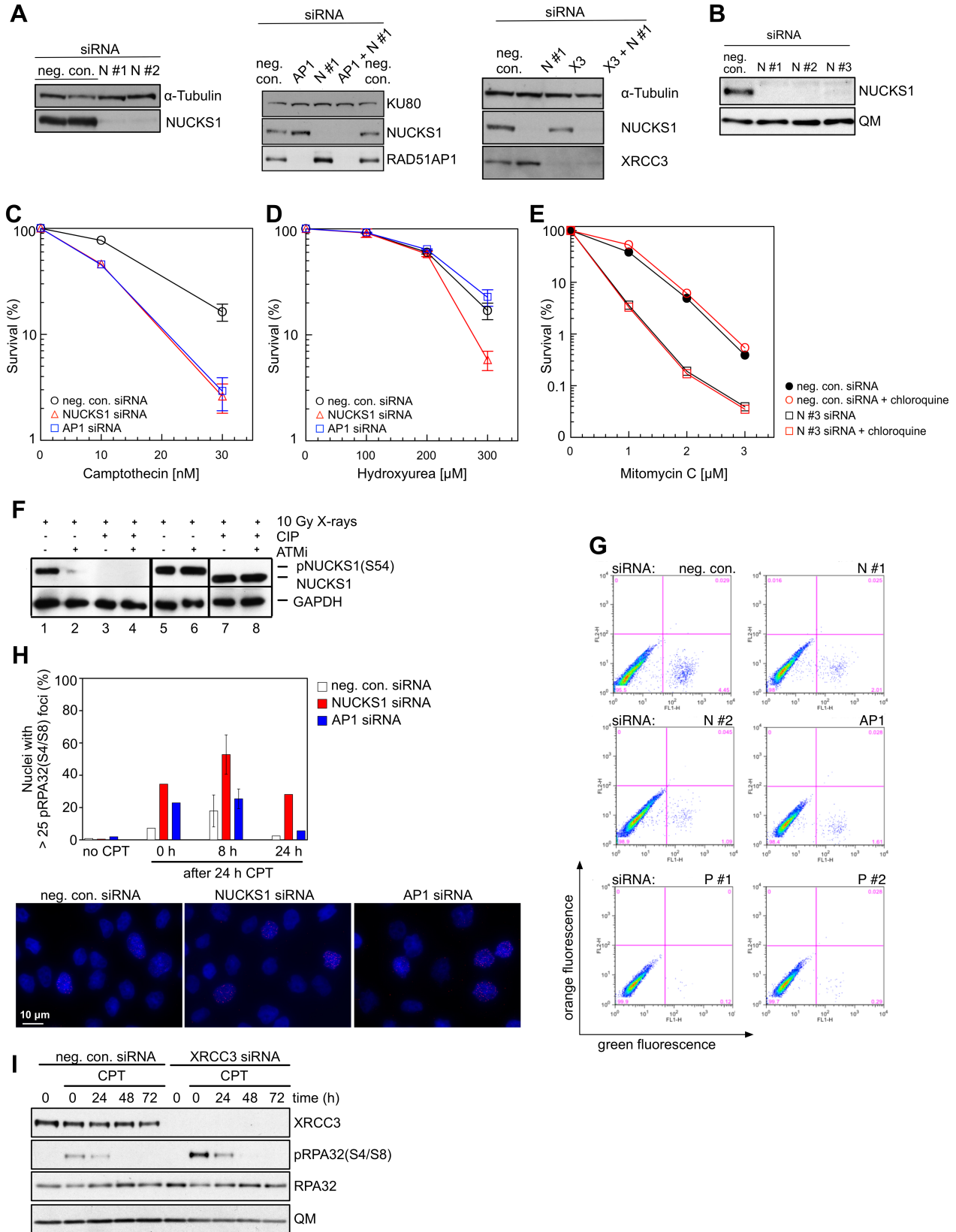
Homo sapiens      SDEFFLMEDDDSDYGSSKKKNKMVKS---KPERKEKMPKPRLKATVTPSPVKGKGVGRPTASKASKEKTPSP-----
Mouse            SDEFFLMEDDDSDYGSSKKNQKMVKS---QPERKEKEMPQPRVKATVTPSPVKGQAKVGRPTASKKSKETPSP-----
Chinese hamster  SDEFFLMEDDDSDYGSSKKKNKKSKS---KPERKEKMPKPRLKATVTPSPVKGKAGRPTASKTKETPSP-----
African clawed frog SDEFFMVEDDDSDYGRSKKK-KKIVKS---KPERKEKRVPKPRLKATVTPSPVKAKGS-RPAASKAPKEKSPSPKA-----EEE
Pufferfish      SDEFFMVEDDDSDYQSKKRGKVIRRG---RPDKKERKSPKPRLKATVTPSPMKGKGRPTAKLEKSSPKEEEEEDPESPLEEEE
Zebrafish       SDEFFMVEDDDSDYGHSKKKGVVPRGGRRVEKKEKSPKPRLKATVNPSPMKGKGRPSAAKALEKSSPKDEEEESP---AEDEE

Homo sapiens      KEEDEEPESPPEKTSTSP-----PEKSGDEGESEDEAPSGED
Mouse            QEEDEEAESPEKK-----SGDEGESEDEASSGED
Chinese hamster  KEEDEEPESPPEKKSASPP-----PEKSGDEGESEEEAPSGED
African clawed frog EEEDEEPVTPPEKKSTSP-----QEKSGDDVSEEAQSTED
Pufferfish      EEEAEKKETSPAPTKEAAGDEEEDEEEDEEGEEEAPSGED
Zebrafish       EDEVEKKESPPSKKTKDEAP---EDEEEDEEEDEGEEEAPSGED

```

**Supplementary Fig. S1:** ClustalW sequence alignment of the NUCKS1 protein family to show that NUCKS1 orthologs are present across vertebrates. Acidic residues are in red, basic residues are in blue. The putative DNA-binding domain identified in human NUCKS1 using a synthetic peptide containing an extended GRP-motif (1) is shown in grey, with the GRP sequence underlined in black. NUCKS1 orthologs do not appear to be present in invertebrates or in any model simple organisms, such as *D. melanogaster*, *C. elegans* or yeast.

**Supplementary Figure S2**



**Supplementary Fig. S2:** (A) Representative Western blots showing the level of protein depletion for the experiments carried out in Figure 2A. The signals for  $\alpha$ -Tubulin and for KU80 serve as loading

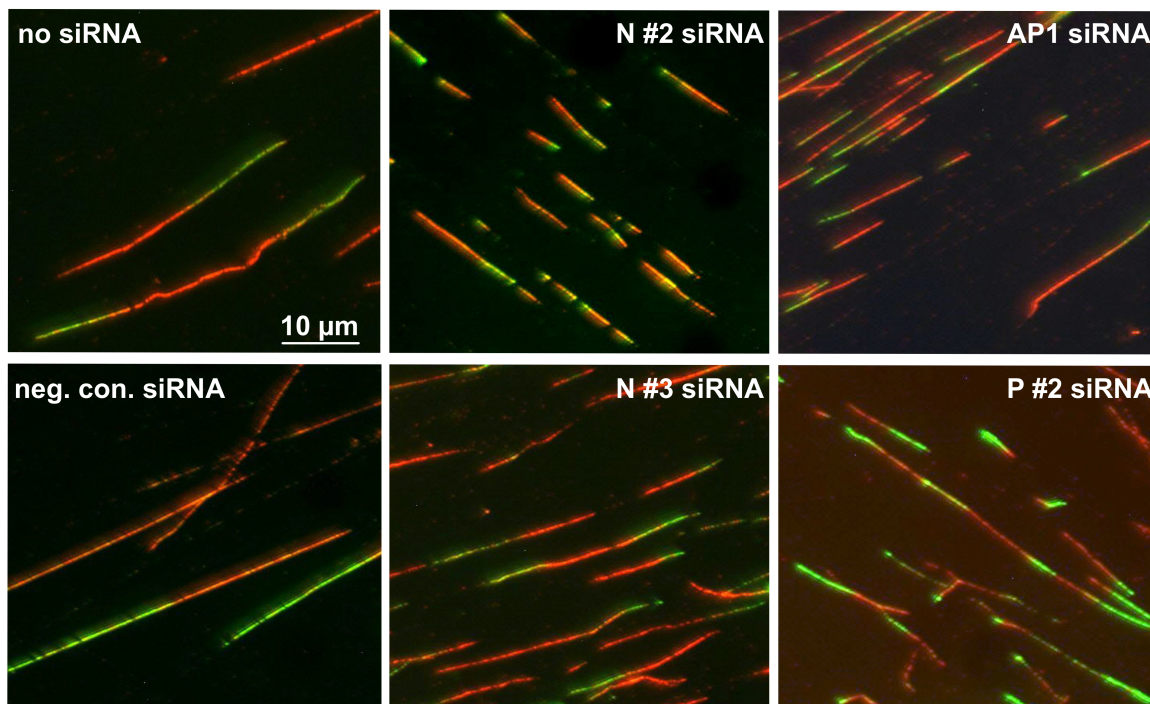
controls. (B) Western blot to show the extent of protein depletion for the three NUCKS1-targeting siRNAs used in this study. QM serves as loading control. (C) Results from colony formation assays to show that NUCKS1 knockdown sensitizes HeLa cells to the cytotoxic effects of camptothecin (CPT). The results for RAD51AP1 knockdown are shown for comparison purposes. Data with error bars are the mean from 2 independent experiments  $\pm$  SD. (D) Results from colony formation assays to show that NUCKS1 knockdown sensitizes HeLa cells to the cytotoxic effects of 300  $\mu$ M hydroxyurea (HU) treatment. The results for RAD51AP1 knockdown are shown for comparison purposes. Data with error bars are the mean from 2 independent experiments  $\pm$  SD. (E) Cell survival curves obtained after MMC exposure of HeLa cells transfected with neg. con. siRNA or with NUCKS1-depleting siRNA #3, with or without pre-incubation (2 h) in 20  $\mu$ g/ml chloroquine, as indicated. (F) Western blots to show that phosphorylated NUCKS1 at serine 54 (using  $\alpha$ -pNUCKS1(S54) antibody) is detectable in DNA-PK-deficient M059J cells 1 h post exposure to 10 Gy X-rays (lanes 1, 5 and 6). Treatment of M059J extracts with calf intestinal phosphatase (CIP; NewEngland Biolabs) removes the specific band detected by the  $\alpha$ -pNUCKS1(S54) antibody (lanes 3 and 4), as does pre-treatment with the ATM inhibitor (lane 2). Note: CIP removes many phosphorylation sites in NUCKS1, which leads to a mobility shift (compare lanes 5 and 6 to lanes 7 and 8). Lanes 1-4: probed to  $\alpha$ -pNUCKS1(S54) antibody; lanes 5-8: probed to  $\alpha$ -NUCKS1 antibody. GAPDH serves as loading control. (G) Representative analysis of GFP fluorescence in U2OS-DR cells transfected with negative control siRNA (neg. con.), depleted for NUCKS1 by one of two different siRNAs (#1 or #2), depleted for RAD51AP1 (AP1), or depleted for PALB2 by one of two different siRNAs (P #1 or P #2). Two-color fluorescence analysis was performed with the percentage of green cells indicated at the bottom of each lower right panel. FL1-H: green fluorescence; FL2-H: orange autofluorescence. (H) Upper panel: Fraction of nuclei with >25 pRPA32(S4/S8) foci following camptothecin washout in NUCKS1-depleted HeLa cells compared to control cells (neg. con. siRNA). The results for RAD51AP1 knockdown are shown for comparison purposes. Bars without error bars are the mean from 2 independent experiments. Bars with error bars are the mean from 3 independent experiments  $\pm$  SEM. Lower panel: Representative micrographs obtained for the conditions tested above at 8 h post CPT washout. pRPA(S4/S8) foci: red; DAPI: blue. (I) Representative western blots obtained for the camptothecin washout experiments described in Figure 4 of the main manuscript using U2OS control cells and U2OS cells depleted for XRCC3. The signal for QM serves as loading control.

**Supplementary Figure S3**

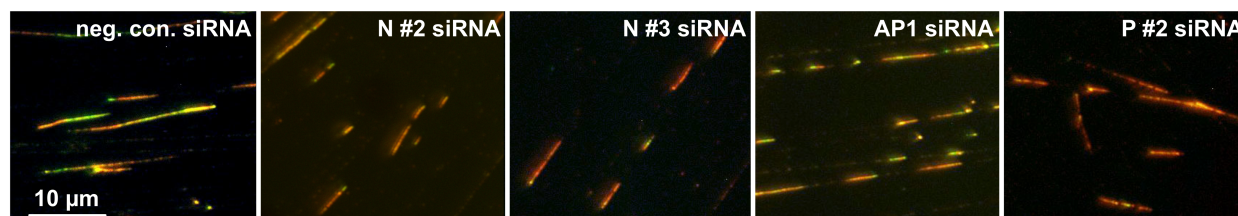
**A**



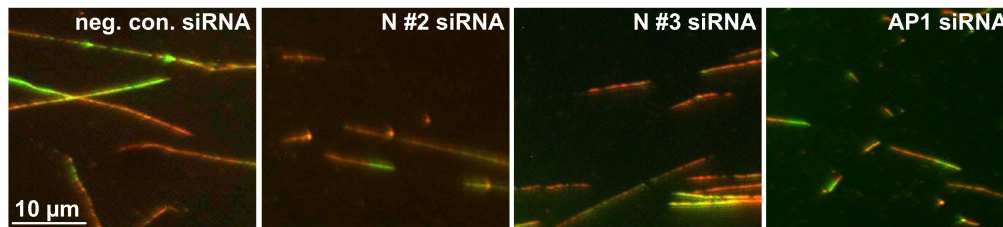
**B**



**C**



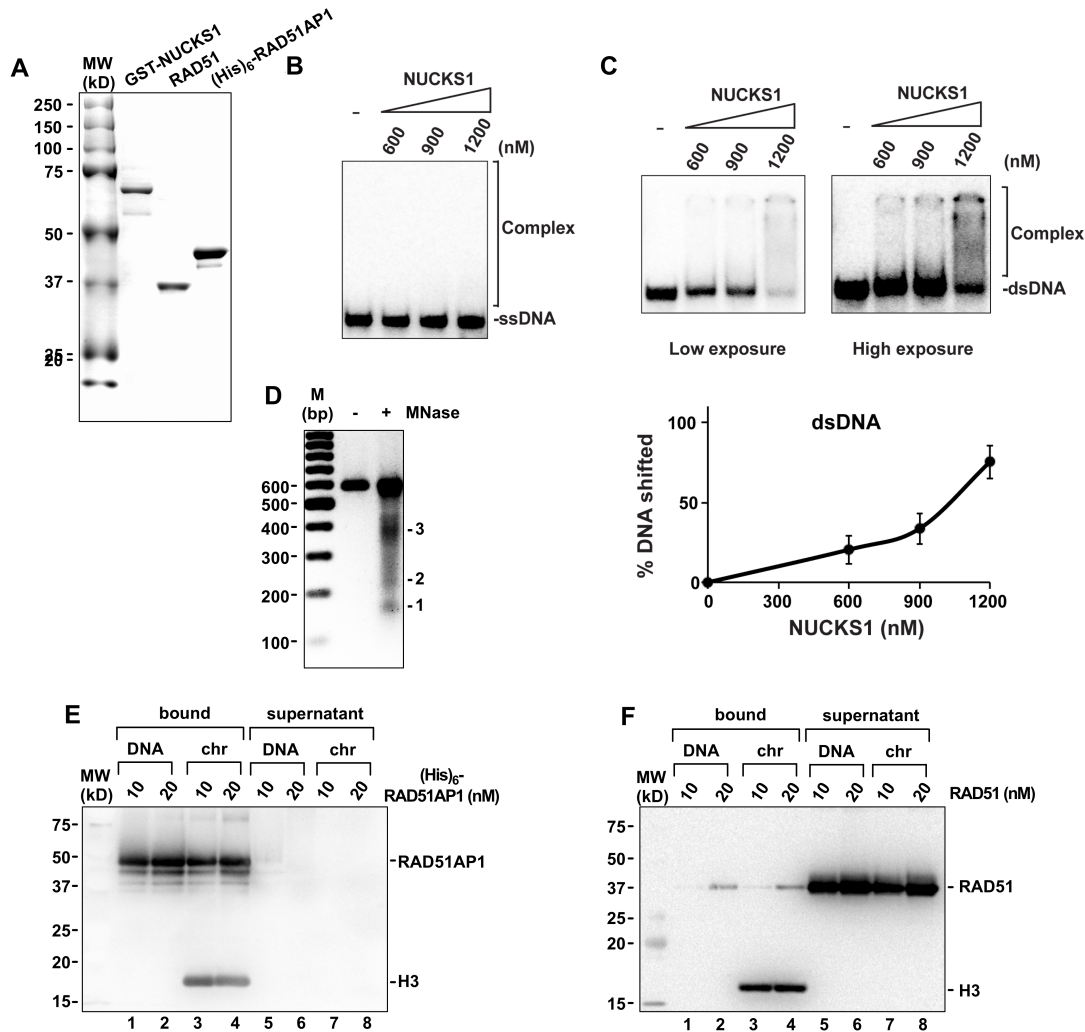
**D**



**Supplementary Fig. S3:** (A) Representative western blots to assess the extent of protein knockdown for the experiments described in Figure 5 and Figure 6 of the main manuscript. The signals for QM

and KU80 serve as loading controls. SiRNAs as indicated: NUCKS1 siRNAs: N #2 and N #3; RAD51AP1 siRNA: AP1; control siRNA: neg. con., PALB2 siRNAs: P #1 and P #2; - : no siRNA in transfection. (B) Representative micrographs of DNA fibers obtained from U2OS cells under conditions of unperturbed DNA replication and transfected with siRNAs, as indicated. Red: CldU; green: IdU. (C) Representative micrographs of DNA fibers obtained from U2OS cells after a 30 min treatment with 2 mM HU, as described in Figure 6A, and transfected with siRNAs, as indicated. Red: CldU; green: IdU. (D) Representative micrographs of DNA fibers obtained from U2OS cells after a 30 min treatment with 0.5  $\mu$ M TPT, as described in Figure 6D, and transfected with siRNAs, as indicated. Red: CldU; green: IdU.

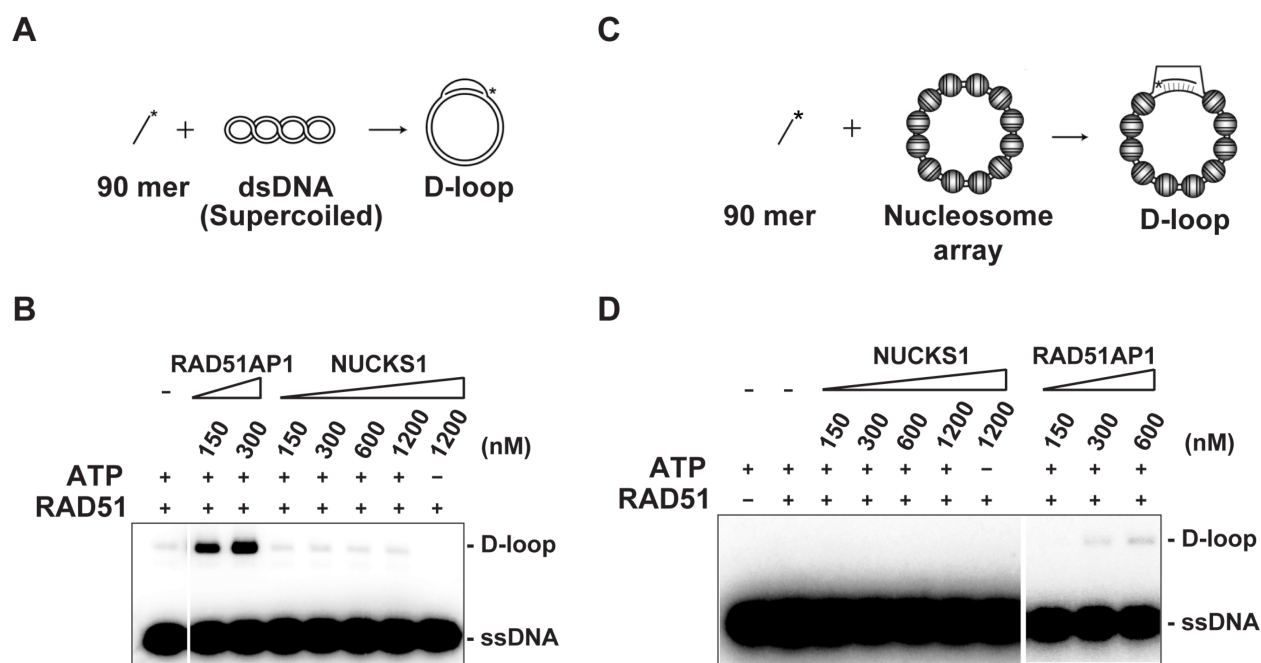
### Supplementary Figure S4



**Supplementary Fig. S4:** NUCKS1 binds to dsDNA but not to ssDNA and, unlike NUCKS1, neither RAD51AP1 nor RAD51 prefer binding to chromatin over naked DNA. (A) SDS-PAGE to show recombinant proteins used here: GST-NUCKS1, RAD51 and (His)<sub>6</sub>-RAD51AP1. (B) GST-NUCKS1 (0.6-1.2  $\mu$ M) was incubated with ssDNA (2.5 nM; same substrate as shown in Figure 7A of the main manuscript) and analyzed for mobility shifts using an 8% polyacrylamide gel. (C) GST-NUCKS1 (0.6-1.2  $\mu$ M) was incubated with dsDNA (2.5 nM; same substrate as shown in Figure 7A of the main manuscript) and analyzed for mobility shifts using an 8% polyacrylamide gel (upper panels). The results from the quantified mobility shifts were plotted (lower panel). Data points are the means from 3 independent experiments  $\pm$  1SD. (D) Agarose gel to show the results of the MNase digest of the biotinylated 588 bp chromatinized dsDNA fragment. Positions of 1, 2 and 3 histone octamers as indicated. (E) Western blot obtained after immobilized DNA pull-down assays using either naked

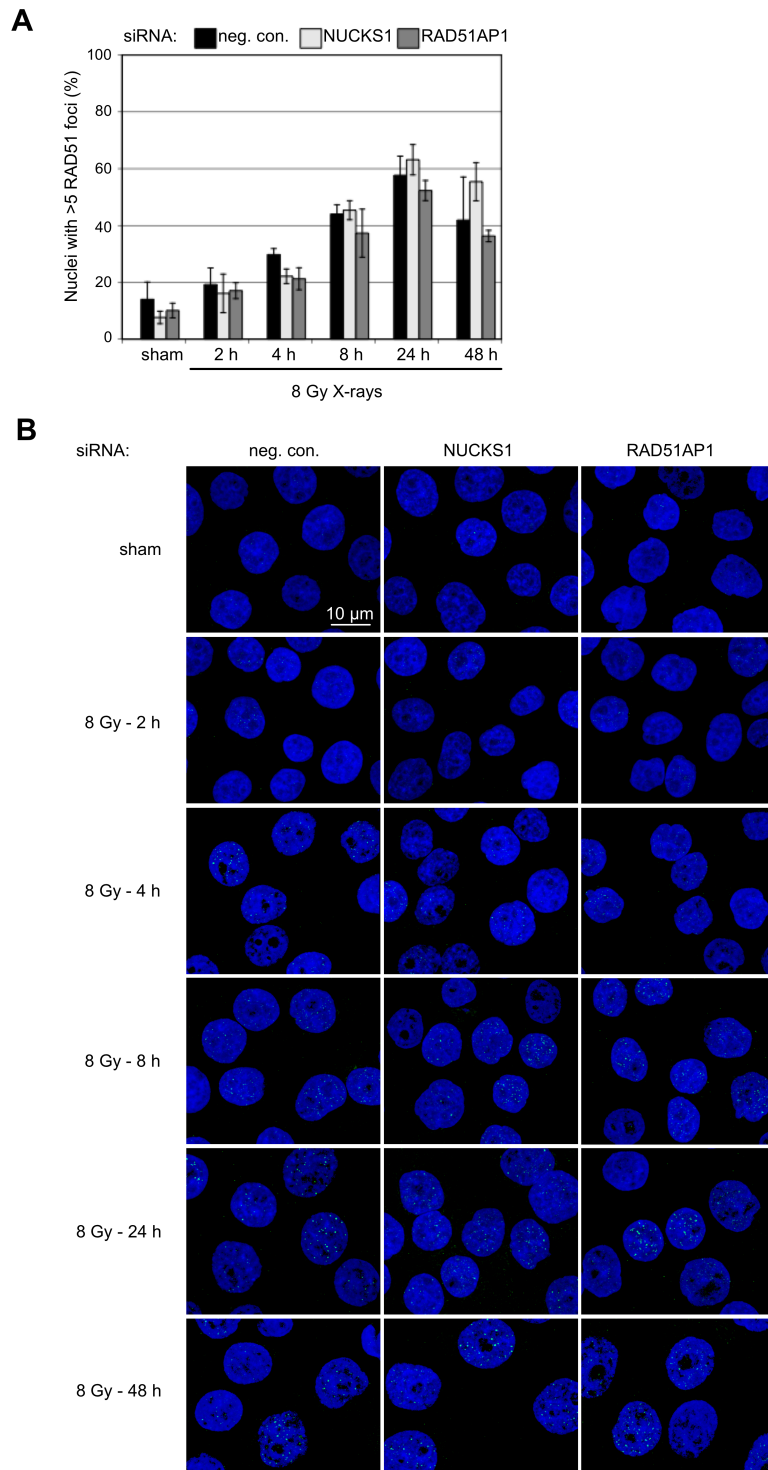
DNA (here: DNA (50 nM/reaction)) or chromatinized DNA (here: chr (50 nM/reaction)) and 10 or 20 nM (His)<sub>6</sub>-RAD51AP1, as indicated. DNA-bound (His)<sub>6</sub>-RAD51AP1 (lanes 1-2), chromatin-bound (His)<sub>6</sub>-RAD51AP1 (lanes 3-4), and unbound (His)<sub>6</sub>-RAD51AP1 in the supernatants from the reactions in lanes 1-4 (lanes 5-8, respectively). The signal for histone H3 (here: H3) serves as control for successful chromatinization (lanes 3-4) and shows that histones are not disrupted (no H3 signal in lanes 7-8). (F) Western blot obtained after immobilized DNA pull-down assays using either naked DNA (here: DNA (50 nM/reaction)) or chromatinized DNA (here: chr (50 nM/reaction)) and 10 or 20 nM RAD51, as indicated. DNA-bound RAD51 (lanes 1-2), chromatin-bound RAD51 (lanes 3-4), and unbound RAD51 in the supernatants from the reactions in lanes 1-4 (lanes 5-8, respectively). The signal for histone H3 (here: H3) serves as control for successful chromatinization (lanes 3-4) and shows that histones are not disrupted (no H3 signal in lanes 7-8).

### Supplementary Figure S5



**Supplementary Fig. S5: NUCKS1 does not stimulate D-loop formation.** (A) Schematic of the D-loop reaction with naked pBluescript SK plasmid DNA. (B) RAD51AP1 (150 nM or 300 nM) and NUCKS1 (150 nM, 300 nM, 600 nM or 1200 nM) were tested for their ability to promote RAD51 mediated D-loop formation with naked pBluescript SK plasmid. (C) Schematic of the D-loop reaction with chromatinized pBluescript SK plasmid. (D) NUCKS1 (150 nM, 300 nM, 600 nM or 1200 nM), and RAD51AP1 (150 nM, 300 nM or 600 nM) were tested for their ability to promote RAD51 mediated D-loop formation with chromatinized pBluescript SK plasmid DNA.

## Supplementary Figure S6



**Supplementary Figure S6:** (A) Kinetics of RAD51 foci formation in control cells HeLa (sham) and in HeLa cells exposed to 8 Gy X-rays. SiRNAs are as indicated. For the depletion of NUCKS1 a cocktail of NUCKS1 siRNAs (N #1, N #2 and N 3#) was used. (B) Representative micrographs obtained for the time points assessed in A. Green: RAD51, blue: DAPI.

## Supplementary Methods

### Microscopy of pRPA(S4/S8) foci and image analysis

For image capture of pRPA(S4/S8) foci, 10 Z-stack section images were taken per sample each consisting of 24 stacks (0.3  $\mu\text{m}$  intervals) using a 63 $\times$  oil objective and a Zeiss Axio-Imager.Z2 microscope equipped with Metamorph software (Molecular Devices, Sunnyvale, CA). Z-stacks were collapsed down to the maximum intensity projections and a combination of ImageJ (<http://rsb.info.nih.gov/ij/>) and Cell Profiler (<http://www.cellprofiler.org/>) software programs was used with the following custom program settings for image processing: minimum object size = 3; maximum object size = 35; despeckle ratio = 0.3; rolling ball size = 5. A custom-built pipeline for automated cell (80 – 300 pixel units) and pRPA(S4/S8) foci counting with settings for shape (*i.e.* 0.5) and dimensions (*i.e.* 5 pixels diameter) was employed. Foci detected were first normalized to their respective control samples (sham treated) and counted as positive nuclei only, if they had >25 foci/nucleus.

### Chromatinized template

Chromatin was assembled with the purified human histone octamer and pBluescript SK dsDNA by the salt dialysis method as described (2). Chromatin assembly was monitored by EMSA, micrococcal nuclease digestion, and accessibility to the restriction enzyme HaeIII (3,4).

### D-loop reaction

The D-loop reaction was carried out as described previously (5,6). Briefly,  $^{32}\text{P}$ -labeled 90-mer oligonucleotide (2.4  $\mu\text{M}$  nucleotides) was preincubated with RAD51 (1  $\mu\text{M}$ ) for 5 min at 37°C in the reaction buffer E (25 mM Tris-HCl, pH 7.5, 60 mM KCl, 1 mM DTT, 1 mM  $\text{MgCl}_2$ , 1 mM  $\text{CaCl}_2$ , 2 mM ATP, and 100  $\mu\text{g}/\text{ml}$  BSA). This was followed by the incorporation of RAD51AP1 or NUCKS1 and a 5-min incubation at 37°C. The D-loop reaction was initiated by adding naked or chromatinized pBluescript SK replicative form I DNA (37  $\mu\text{M}$  base pairs) and incubated at 37°C for 7 min. The molar ratio of the 90-mer to pBluescript plasmid in the reactions was 2.1 to 1. After electrophoresis in a 1% agarose gel, phosphorimaging analysis was carried out to visualize the radiolabeled DNA species (6).

### Micrococcal Nuclease digestion of the biotinylated 588 bp DNA fragment

The Micrococcal Nuclease (MNase) digestion assay was performed on chromatin assembled by salt dilution in 1:3 ratio of DNA:Octamer (pmole:pmole), and according to the instructions by the manufacturer (New England BioLabs). Briefly, 500 ng of chromatin assembled on the biotinylated 588 bp DNA fragment were incubated with 10 units of MNase in 1X MNase buffer at 37°C. Following the incubation times (as indicated), MNase was immediately inhibited by adding 10  $\mu\text{l}$  TE:EDTA (1XTE:250 mM EDTA) buffer. Samples were deproteinized by incubation with 2.5  $\mu\text{g}$  proteinase K in buffer containing 20 mM EDTA, 200 mM NaCl and 1% SDS at 37°C for 30 min. MNase digested DNA was purified by phenol/chloroform/isoamylalcohol extraction and ethanol precipitated. DNA fragments were analyzed on a 1.5% agarose gel and visualized by ethidium bromide.

## Supplementary References

1. Grundt, K., Skjeldal, L., Anthonsen, H.W., Skauge, T., Huitfeldt, H.S. and Ostvold, A.C. (2002) A putative DNA-binding domain in the NUCKS protein. *Arch Biochem Biophys*, 407, 168-175.
2. Stein A. (1989) Reconstitution of chromatin from purified components, *Methods Enzymol*, 170, 585–603.
3. Alexiadis V., Kadonaga J.T. (2002) Strand pairing by Rad54 and Rad51 is enhanced by chromatin. *Genes Dev*, 16, 2767–2771.
4. Lusser A., Kadonaga J.T. (2004) Strategies for the reconstitution of chromatin. *Nat. Methods*, 1, 19–26.



5. Zhao W., Saro D., Hammel M., Kwon Y., Xu Y., Rambo R.P., Williams G.J., Chi P., Lu L., Pezza R.J., *et al.* (2014) Mechanistic insights into the role of Hop2-Mnd1 in meiotic homologous DNA pairing. *Nucleic Acids Res*, 42, 906-917.
6. Chi P., Van Komen S., Sehorn M.G., Sigurdsson S., Sung P. (2006) Roles of ATP binding and ATP hydrolysis in human Rad51 recombinase function. *DNA Repair (Amst.)*, 5, 381-391.